

Dephasing in coherently-split quasicondensates

H.-P. Stimming¹, N. J. Mauser¹, J. Schmiedmayer², I. E. Mazets^{1,2,3}

¹Wolfgang Pauli Institute c/o University of Vienna, 1090 Vienna, Austria

²Vienna Center for Quantum Science and Technology, Atominstut, TU Wien, 1020 Vienna, Austria

³Ioffe Physico-Technical Institute, 194021 St.Peterburg, Russia

We numerically model the evolution of a pair of coherently split quasicondensates. A truly one-dimensional case is assumed, so that the loss of the (initially high) coherence between the two quasicondensates is due to dephasing only, but not due to the violation of integrability and subsequent thermalization (which are excluded from the present model). We confirm the subexponential time evolution of the coherence between two quasicondensates $\propto \exp[-(t/t_0)^{2/3}]$, experimentally observed by S. Hofferberth *et. al.*, Nature **449**, 324 (2007). The characteristic time t_0 is found to scale as the square of the ratio of the linear density of a quasicondensate to its temperature, and we analyze the full distribution function of the interference contrast and the decay of the phase correlation.

PACS numbers: 03.75.Gg, 03.75.Kk

I. INTRODUCTION

Dephasing and decoherence are phenomena at the heart of many-body physics which are deeply related to such fundamental problems as the crossover between quantum and classical dynamics of complex systems [1], reversibility of physical processes [2] or quantum information storage and processing [3]. To better understand dephasing and decoherence phenomena, we need systems, which are, on one hand, simple and theoretically tractable, but, on the other hand, available experimentally. In particular, ultracold, weakly-interacting bosonic atoms offer such an opportunity. In the present paper, we investigate numerically the time-dependent dephasing of ultracold atomic systems.

A system of identical bosons confined to one-dimensional (1D) geometry is experimentally realizable with ultracold atoms trapped on atom chips [4] or in an array of tight waveguides formed by a 2D optical lattice [5]. The conditions of one-dimensionality are smallness of the temperature with respect to the energy quantum $\hbar\omega_r$ of the radial (harmonic) Hamiltonian,

$$k_B T \ll \hbar\omega_r, \quad (1)$$

and smallness of the product of the 3D s -wave atomic scattering length a_s and the mean linear density n_{1D} ,

$$n_{1D} a_s \ll 1. \quad (2)$$

A 1D system of identical bosons interacting via contact pairwise potential is describable in the second quantization representation by the Hamiltonian

$$\hat{H} = \int dz \left(\frac{\hbar^2}{2m} \frac{\partial \hat{\psi}^\dagger}{\partial z} \frac{\partial \hat{\psi}}{\partial z} + \frac{g_{1D}}{2} \hat{\psi}^\dagger \hat{\psi}^\dagger \hat{\psi} \hat{\psi} \right), \quad (3)$$

where m is the mass of the boson, $\hat{\psi} = \hat{\psi}(z, t)$ is the bosonic annihilation field, and g_{1D} is the effective coupling strength of the 1D contact interaction (in what follows we assume repulsive interaction, $g_{1D} > 0$). The

system described by this Hamiltonian supplemented by periodic boundary conditions is known to be fully integrable with the ground state properties and excitation spectrum in the thermodynamic limit given by the well-known Lieb-Liniger model [6].

Recalling that the coupling strength satisfies $g_{1D} = 2\hbar\omega_r a_s$ as long as $a_s \ll l_r \equiv \sqrt{\hbar/(m\omega_r)}$ [7], we see that Eq. (2) requires smallness of the mean interaction energy per particle with respect to $\hbar\omega_r$. Both Eqs. (1) and (2) mean small population of radially excited modes, either by temperature or interaction effects, respectively.

In fact, the radial degrees of freedom are always excited *virtually*, with the excitation amplitude $\sim n_{1D} a_s$. This leads to the emergence of higher-orders in $\hat{\psi}^\dagger \hat{\psi}$ (cubic etc.) terms in Hamiltonian, in addition to what is given by Eq. (3). These terms, corresponding to many-particle (three-particle etc.) effective elastic collisions, violate the integrability and lead to thermalization on the time scale, at longest, $\sim 1/[\omega_r (n_{1D} a_s^2 / l_r)^2]$ [8]. Virtual radial mode excitations have been studied even earlier, in the context of soliton decay [9] or quasi-1D (macroscopic) flow of a degenerate bosonic gas through a waveguide [10]. However, here we neglect this effect in order to study purely integrable dynamics.

In what follows, we consider uniform ($n_{1D} = \text{const}$ for all z) and weakly interacting ($mg_{1D}/\hbar^2 \ll n_{1D}$) systems, $n_{1D} = \langle \hat{\psi}_j^\dagger(z, t) \hat{\psi}_j(z, t) \rangle$ being the mean linear density of bosons. For temperatures below $T_{qc} \sim (g_{1D} \hbar^2 n_{1D}^3 / m)^{1/2} / k_B$ [11], a weakly-interacting system of bosons is in the quasicondensate state [12], which means that the operator $\hat{\psi}$ may be replaced by a classical complex-valued field with a phase fluctuating along z (density fluctuations in the practically important long-wavelength range are suppressed via interactions). In this regime, not only the phase coherence is maintained, but also the density-density correlation function at zero distance approaches 1 (instead of 2, the value characteristic for a non-degenerate bosonic gas) [11]. The stationary

two-point correlation function of a quasicondensate at a finite temperature is [13]

$$\langle \hat{\psi}_j^\dagger(z, t) \hat{\psi}_j(z', t) \rangle = n_{1D} \exp(-|z - z'|/\lambda_T), \quad (4)$$

where the thermal phase-correlation length is

$$\lambda_T = 2\hbar^2 n_{1D} / (mk_B T). \quad (5)$$

Quantum noise is dominant on length scales shorter than $\lambda_T [mg_{1D}/(\hbar^2 n_{1D})]^{1/2} \ll \lambda_T$ [14]. Finite-temperature fluctuations in degenerate bosonic gases in highly anisotropic traps has been extensively studied both theoretically [15, 16] and experimentally [17, 18].

One of the fundamental questions related to the Lieb-Liniger model is: how fast will two mutually decoupled quasicondensates with equal mean linear densities n_{1D} decohere, if their initial fluctuations are highly correlated $\langle \hat{\psi}_1^\dagger(z, 0) \hat{\psi}_2(z, 0) \rangle \approx n_{1D}$? Each of the quasicondensates has (upon tracing out the variables of another one) a finite temperature T . The measure of coherence will be the coherence factor

$$\Psi(t) = \langle \text{Re}\{ \exp[i(\varphi_1(z, t) - \varphi_2(z, t) - \theta_{ov}(t))] \} \rangle, \quad (6)$$

where $\varphi_j(z, t)$ are the local phase operators for the condensate labeled j . By $\theta_{ov}(t)$ we denote the constant overall phase of the system (the phase associated with the Goldstone mode) defined by $\theta_{ov}(t) = 2\omega_r a_s \int_0^t dt' \int_0^L dz [|\psi_2(z, t')|^4 - |\psi_1(z, t')|^4]$ which was described by Lewenstein and You [19] (with L the total length of the condensate). From now on, we replace operators $\hat{\psi}_1, \hat{\psi}_2$ by complex random functions ψ_1, ψ_2 , whose fluctuations account for thermal noise.

We use “operational” definition (6) of the coherence factor on the two reasons: (1) density fluctuations are suppressed by interatomic repulsion and therefore Eq. (6) is practically equivalent to the more traditional definition $\Psi(t) = n_{1D}^{-1} \langle \psi_2^*(z, t) \psi_1(z, t) e^{-i\theta_{ov}(t)} \rangle$ (accounting for the correction to the overall phase); (2) in a time-of-flight interference experiment, the relative phase is directly measured, while the density fluctuations are much harder to detect. We retain the symbol of the real part in Eq. (6), because (i) the imaginary part of the expression in curly brackets becomes exactly zero only after averaging over an infinite ensemble of realization and is small but finite for real experimental data; (ii) we want to be consistent with the notation of Refs. [20, 21].

The phase and density fluctuations in a quasicondensate are calculated from the harmonic approximation to the exact Hamiltonian (3). In the harmonic approximation, fluctuations are Gaussian with zero mean, and, hence, Eq. (6) reduces to

$$\Psi(t) = \exp \left\{ -\frac{1}{2} \langle [\varphi_1(z, t) - \varphi_2(z, t) - \theta_{ov}(t)]^2 \rangle \right\}. \quad (7)$$

In experiment [22], a subexponential decay of coherence

$$\Psi(t) \approx \exp[-(t/t_0)^\alpha] \quad (8)$$

has been detected, with the numerical value of α statistically consistent with the hypothesis

$$\alpha = 2/3. \quad (9)$$

Initially there was a single quasicondensate of ^{87}Rb atoms at the temperature T_{in} between 82 nK and 175 nK. Then it was coherently split into two quasicondensates with the density n_{1D} each (the values of n_{1D} were in the range from $20 \mu\text{m}^{-1}$ to $52 \mu\text{m}^{-1}$). The splitting was made as adiabatic as possible, so that the initial fluctuation in both quasicondensates just after their full separation were almost identical. However, the coherence factor then decayed rapidly as the hold time grew, according to Eqs. (8, 9), with $t_0 \sim 0.01$ s, which is an order of magnitude shorter than the expected thermalization scale for a *non-degenerate* system of that density [8]. This obtained t_0 was in a fair agreement with the theory developed by Burkov, Lukin, and Demler [20], which will be briefly described later, under the assumption that the temperature of the two quasicondensates after the splitting was approximately equal to T_{in} . However, the range of parameter variations (the radial trapping frequency was chosen to be either $2\pi \times 3.3$ kHz or $2\pi \times 4.0$ kHz) in Ref. [22] is too narrow to reliably determine the dependence of t_0 on n_{1D} , T , and ω_r .

II. THEORETICAL APPROACHES

The two existing theoretical descriptions [20, 21] of dephasing in 1D quasicondensates share the common basic model but differ in technical tools to solve it. In both cases two quasicondensates, describable by Eq. (3), are separated by a potential barrier wide and high enough to make their tunnel coupling negligible and, hence, their time evolution after splitting fully distinct. These quasicondensates are assumed to have the same mean atomic density and placed in two waveguides with the same radial trapping frequency. The temperature is low enough ($k_B T \lesssim \mu \equiv 2\hbar\omega_r n_{1D} a_s$) to consider only phononic part of the elementary excitation spectrum. Although static Eqs. (4, 5) hold also for $k_B T > \mu$, the dynamic theories of Refs. [20, 21] rely on the phononic type of the elementary excitations spectrum. In the case $k_B T > \mu$ thermally populated particle-like modes contribute to the system dynamics, and we expect therefore a deviation of the low of coherence factor decay from the theoretical predictions [20, 21].

The quantum noise is fully ignored, and excitations are represented by small-amplitude classical waves. Initially the fluctuations in the both quasicondensates are almost perfectly correlated (initial small interwell fluctuations serve as a seed noise, whose detailed properties are not “remembered” by the system in the long-time asymptotic regime and thus do not affect the final result).

The theory by Burkov, Lukin, and Demler [20] was based on derivation of a Langevin-type equation with the random source term correlation and damping-term

properties described by a certain kernel obtained by re-summation of diverging diagrams describing the exchange of quasiparticles between symmetric ($\hat{\psi}_+ = (\hat{\psi}_1 + \hat{\psi}_2)/\sqrt{2}$) and antisymmetric ($\hat{\psi}_- = (\hat{\psi}_1 - \hat{\psi}_2)/\sqrt{2}$) modes. Finally, Burkov, Lukin, and Demler obtained Eqs. (8, 9) with $t_0 = t_0^{\text{BLD}}$,

$$t_0^{\text{BLD}} = 2.61 \pi \hbar \mu \mathcal{K} / (k_B T)^2, \quad (10)$$

where $\mathcal{K} = \pi \sqrt{\hbar n_{1D} / (2\omega_r a_s)}$ is the Luttinger-liquid parameter of the system. Initially, the symmetric mode is mostly populated, its initial temperature being $T_+|_{t=0} \approx 2T$, and only very small number of excitations are present in the antisymmetric mode, because of slightly nonadiabatic splitting. At large t , the temperatures of two modes equalize, $T_+ \approx T_- \approx T$. Thus, in a strict sense, Ref. [20] reproduces Eqs. (8, 9) in the long-time asymptotic limit only, although in experiment this subexponential coherence decay law was observed even for $t < t_0$.

The Burkov, Lukin, and Demler theory has, although, a weak point: it predicts overdamping of modes with energies larger than $\mu^2 / (k_B T \mathcal{K})$. The damping rate of such modes is of the order of or larger than their frequency. Probably, this result is associated with a possible technical overestimation of the re-summed divergent series. It also may stem from the assumption of the purely linear dispersion law for elementary excitations [20] that provides a large phase space available for products of a splitting of one phonon in the $+$ mode to two phonons in the $-$ mode. However, higher order corrections to the linear phononic dispersion law make this process energetically forbidden in 1D via a small but unavoidable energy mismatch. Neglecting the latter fact may also results in obtaining too fast dynamics of the system. This motivated us to reconsider the problem and to put forward an alternative explanation of the subexponential dephasing.

We refer a reader to our previous paper [21] for the details of the calculations, which are briefly summarized below. We considered motion of pairs of compact wave packets of phonons (with the localization size of the order of the carrier wavelength $2\pi/k$) in two random 1D media with relative fluctuations of local parameters (density and flow velocity) and follow their mutual dephasing, ascribing the obtained dephasing rate to the elementary mode with the momentum $\hbar k$. The source of mutual dephasing is the dependence of the phonon frequency ω_k on the local density δn and flow velocity δV fluctuations:

$$\omega_k = \left(c + \frac{dc}{dn_{1D}} \delta n + \delta V \right) |k|, \quad (11)$$

where $c = \sqrt{\mu/m} \propto \sqrt{n_{1D}}$ is the speed of sound. Then we assume that the contribution into the right-hand-side of Eq. (11) comes only from fluctuations with the wavelength longer than $2\pi/k$ (the influence of short-range fluctuations is averaged out). In other words, a propagating wave packet “sees” the fluctuations only on the length scales longer than its carrier wavelength.

We calculate the statistical properties (the local correlation function at two different instants of time) of the *differences* of the fluctuations related to the 1st and 2nd quasicondensates, i.e., of $\delta n_1 - \delta n_2$ and $\delta V_1 - \delta V_2$ in the limit of asymptotically long time, when the symmetric and antisymmetric modes mostly equilibrate. The estimation for the dephasing rate Γ_k for the two wave packets with the momentum $\hbar k$ propagating in two parallel quasicondensates gives

$$\begin{aligned} \Gamma_k &\sim c|k| \left[\frac{5}{8} \int_{-k}^k \frac{dk'}{2\pi} \frac{k_B T}{\mu n_{1D}} \right]^{1/2} \\ &= \varsigma \sqrt{\frac{k_B T}{m n_{1D}}} |k|^{3/2}. \end{aligned} \quad (12)$$

Here we estimate $\varsigma \approx \sqrt{5/(8\pi)} \approx 0.446$. This estimation stems from our sharp-cutoff assumption. A different model, using some smooth function to eliminate the influence of modes with momenta $\gg \hbar k$, would give another value for ς . However, later we shall see that $\varsigma \approx 0.446$ is quite a reasonable value.

Note that Eq. (12) does not predict overdamping of the modes with the energies close to $k_B T \lesssim \mu$: their damping rate is less than their frequency by a factor $\sim \mathcal{K}$.

The shorter the wavelength of a mode, the faster this mode equilibrates. The integrated coherence factor is then

$$\Psi(t) = \exp \left\{ -\frac{m k_B T}{2\pi \hbar^2 n_{1D}} \int_{-\infty}^{\infty} dk k^{-2} [1 - \exp(-\Gamma_k t)] \right\}. \quad (13)$$

Since $\Gamma_k \propto |k|^{3/2}$ we obtain by integration $\Psi(t) = \exp[-(t/t_0)^{2/3}]$ but with $t_0 = t_0^{\text{MS}}$ [21],

$$t_0^{\text{MS}} = \kappa \frac{\hbar^3 n_{1D}^2}{m (k_B T)^2} = \frac{\kappa}{4} \frac{m \lambda_T^2}{\hbar}, \quad (14)$$

where $\kappa \approx 2.85$ if we take $\varsigma = 0.446$. The fact that t_0^{MS} does not depend on c and, hence, on the atomic interaction strength in the limit $\mathcal{K} \gg 1$, seems to be deeply related to the independence of the thermal correlation length λ_T [Eq. (5)] on c in the static regime.

III. NUMERICAL MODEL

We directly simulated the time evolution of two ^{87}Rb quasicondensates by solving (by a split step spectral method [23]) two Gross-Pitaevskii equations with initial conditions chosen randomly corresponding to Bose-Einstein statistics of classical (thermal) excitations in phase and density waves. The local phase ϕ_j and density n_j , $j = 1, 2$, values in the 1st and 2nd condensates are expressed through the respective values for the symmetric and antisymmetric modes (the local velocity is related to the phase as $V_j = (\hbar/m) \partial \phi_j / \partial z$). At $t = 0$ they are

$$\phi_{1,2}(z, 0) = \frac{\phi_+(z, 0) \pm \phi_-(z, 0)}{\sqrt{2}},$$

$$n_{1,2}(z, 0) = n_{1D} + \frac{\delta n_+(z, 0) \pm \delta n_-(z, 0)}{\sqrt{2}}, \quad (15)$$

where the fluctuations for the + and - modes will be specified below.

A. Initial conditions: The splitting process

Exact values of these fluctuations depend on the details of the splitting process and its non-adiabaticity (for example, for the regime of the linear decrease of the tunnel coupling between two quasicondensates the population of phonons in the - mode is expressible via Bessel functions [24]). However, without exact knowledge of the splitting process, we can only give an estimation of the initial fluctuations. In the present paper, we approximate the initial populations of the symmetric and antisymmetric elementary excitation modes by thermal distributions with the temperatures T_+ and $T_- = \eta T_+$, $\eta \ll 1$, respectively. In the course of subsequent evolution, the temperatures of the + and - modes equalize and approach $[(1 + \eta)/2]T_+$.

The particular choice of this parameter ($\eta = 0.1$ in our simulation) and the stability of our results against its variations are discussed in Sec. IV.B.

The initial fluctuations appearing in Eq. (15) are given by

$$\begin{aligned} \delta n_{\pm}(z, 0) &= 2\sqrt{\frac{n_{1D}}{L}} \sum_k \sqrt{S_k} B_k^{\pm} \cos(kz + \zeta_k^{\pm}), \\ \phi_{\pm}(z, 0) &= \frac{1}{\sqrt{n_{1D}L}} \sum_k \frac{1}{\sqrt{S_k}} B_k^{\pm} \sin(kz + \zeta_k^{\pm}), \end{aligned} \quad (16)$$

where $S_k = |k|/\sqrt{k^2 + 4m\mu/\hbar^2}$. Here the sum is taken over $k = 2\pi M_k/l$, where M_k is a non-zero integer number running from $-M_{\max}$ to M_{\max} . The phases ζ_k^{\pm} are uniformly distributed between 0 and 2π and B_k^{\pm} is a positive number whose square has the exponential probability distribution $dP(|B_k^{\pm}|^2)d|B_k^{\pm}|^2 = \langle |B_k^{\pm}|^2 \rangle^{-1} \exp(-|B_k^{\pm}|^2/\langle |B_k^{\pm}|^2 \rangle)$.

In the present paper, we completely neglect the quantum noise (zero-point oscillations of quantized local density and phase), since taking it into account severely limits the time scale of reliable numerical integration of equations of motion of the system in the truncated Wigner approximation [25]. Since we take into account only classical (thermal) excitations, we have:

$$\langle |B_k^{\pm}|^2 \rangle = \frac{k_B T_{\pm}}{\sqrt{\frac{\hbar^2 k^2}{2m} \left(\frac{\hbar^2 k^2}{2m} + 2\mu \right)}}, \quad (17)$$

Here is the difference between our approach and that of Bistritzer and Altman [26], who simulated the dephasing of two quasicondensates with only quantum ($T_- = 0$) fluctuations in the antisymmetric mode at $t = 0$. Using pseudo-random numbers $\xi_{k,1}^{\pm}$ and $\xi_{k,2}^{\pm}$, uniformly distributed between 0 and 1, we obtain the amplitude and

phase of the excitation in a given mode:

$$B_k^{\pm} = \sqrt{\langle |B_k^{\pm}|^2 \rangle |\ln \xi_{k,1}^{\pm}|}, \quad \zeta_k^{\pm} = 2\pi \xi_{k,2}^{\pm}. \quad (18)$$

B. Numerical method

For obtaining reliable random numbers for the choice of initial states, we employ a Pseudo-Random Number generator of Wichmann and Hill [27], implemented here as a 4-fold combined multiplicative congruential generator. We use periodic boundary conditions with a simulation interval length which is of the order of the longitudinal extension of the condensate.

Then the time-dependent Gross-Pitaevskii equation is solved by a 4th-order Fourier Split-Step method, the corresponding time-dependent coherence factor is calculated and then averaged over a large enough sample of random realizations of this simulation. The resolution of the Fourier approximation is chosen such that the maximum energy of the quasiparticle (corresponding to the shortest resolvable wavelength) exceeds $k_B T$, thus preventing the overestimation of the interwell coherence.

We obtained reliable (stable and convergent) results in the parameter range spanning over half an order of magnitude in both the temperature T (from 30 to 100 nK) and the mean densities n_{1D} (from 30 to 100 μm^{-1}) with and additional constraint (to be discussed below): the reliable results were obtained for the density-to-temperature ratio less than or of order of 1 $\text{nK}^{-1} \mu\text{m}^{-1}$, further increase of this ratio resulted in the appreciable dependence of the results on the grid size, which we could not eliminate within the reasonable range of the space and time steps. We also varied the effective 1D coupling strength by increasing the radial trapping frequency from $2\pi \times 3$ kHz to $2\pi \times 9$ kHz. Typical results are shown in Fig. 1.

IV. NUMERICAL RESULTS

A. Full distribution function of interference

In Fig. 2, we illustrate the numerically obtained temporal evolution of the two-condensate joint Full Distribution Function (FDF), in the spirit of Ref. [28]. On polar plots shown in Fig. 2, the polar radius of a point gives the contrast C of the interference fringes *integrated over the sampling length* L_{sam} , and the polar angle is the phase Θ of such an integrated interference pattern. The FDF (in arbitrary units) is shown as a false color density plot.

Locally, the relative phase randomizes rapidly, we can see that from Fig. 2 (a). However, since the correlation length of the phase in each quasi-condensate is λ_T , the contrast does not decrease significantly as long as $L_{\text{sam}} \lesssim \lambda_T$. As we increase the sampling length, the

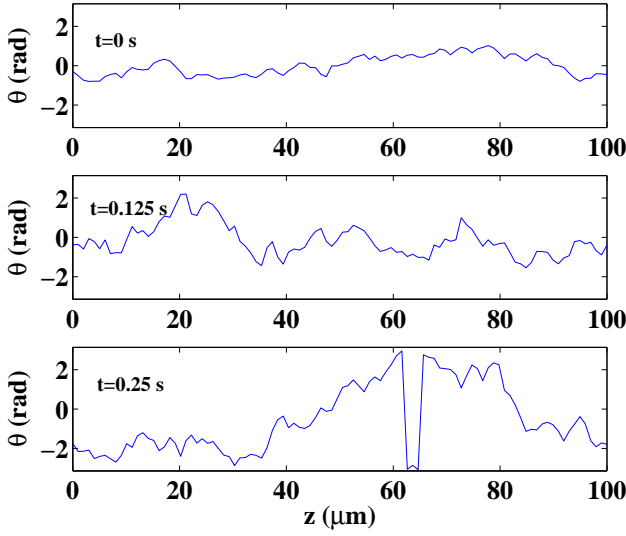


FIG. 1: (Color online). Typical distribution of the relative phase $\theta(z, t) = \phi_1(z, t) - \phi_2(z, t)$ along the quasicondensate axis at several hold times between $t=0$ and $t = 0.25$ s. $n_{1D} = 50 \mu\text{m}^{-1}$, $T_+ = 50$ nK.

local phases become more and more averaged out, and for the parameters of Fig. 2 (b), the contrast C begins to decrease first, and then the distribution of Θ starts to spread. Remarkably, even at times as long as 0.25 s there are still many realizations yielding C close to 1.

Note, that in our analysis we assumed equal mean atom numbers in the two quasicondensate. The splitting process, that always happens in finite time, causes fluctuations of the relative number difference between two wells and, hence, provides an additional mechanism for the global phase diffusion [29, 30]. Experimentally observed [22] high initial phase coherence signifies uncertainty of the interwell atom-number difference (otherwise the overall phase would be completely random). However, the phase diffusion affects only the global phase and not the coordinate-dependent noise and correlation properties. The global phase can be eliminated during the elaboration of experimental data and is therefore not a major hurdle to experimental studies of dephasing.

B. Evaluation of the coherence factor

Evaluating our simulated data, we obtained a subexponential decay of the coherence factor consistent with Eqs. (8, 9) in a wide range of parameters, see Fig. 3.

Before proceeding further, we discuss our choice of the parameter η , the initial ratio of the temperatures in the + and - modes, and the sensitivity of our results to changes of this parameter.

For all the simulations, presented beginning from Fig. 4, we used $\eta = 0.1$. We choose this value because it gives the initial contrast that agrees with the experimental data [22] [$\Psi(0) \approx 0.9$ for a condensate of the length

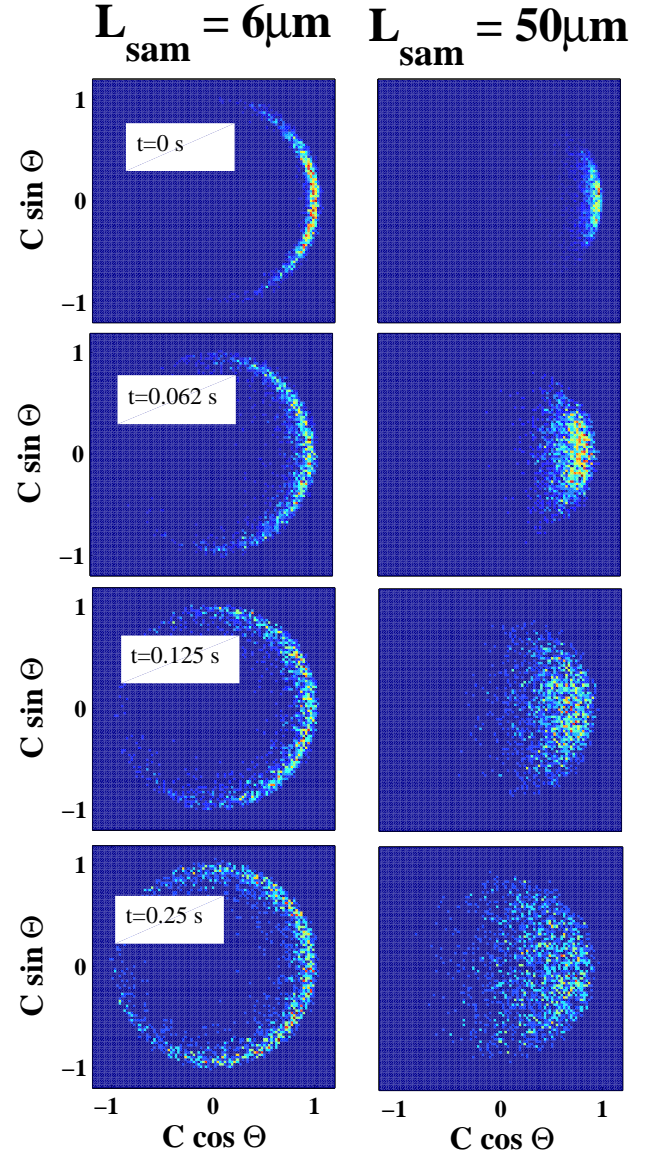


FIG. 2: (Color online). Time evolution of the Full Distribution Function shown as a false-color density plot (dark-blue: zero density; red: maximum density) derived from 3000 numerical runs. $n_{1D} = 50 \mu\text{m}^{-1}$, $T_+ = 50$ nK. Increasing time from top to bottom, times between 0 s and 0.25 s. Sampling length: $L_{\text{sam}} = 6 \mu\text{m}$ for left column, $L_{\text{sam}} = 50 \mu\text{m}$ for right column. Units on the axes are dimensionless.

$\sim 100 \mu\text{m}$]. Anyway, a description of the initial fluctuations beyond our model of thermal fluctuations at the temperature $T_- = \eta T_+$ would require a detailed knowledge of the splitting process.

We checked the sensitivity of our simulations to the choice of the parameter η . A plot of $\ln |\ln \Psi|$ against $\ln t$ is shown in Fig. 3. We can observe that the slope of the sub-exponential decay is varying only slightly. This means that the subexponential decay with $\alpha = 2/3$ is quite insensitive to initial conditions within the given

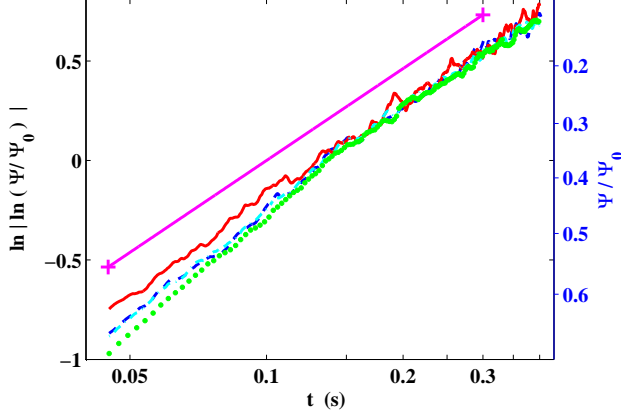


FIG. 3: (Color online). $\ln|\ln \Psi|$ as a function of time for different values of $\eta = \frac{T_-}{T_+}$: $\eta = 0.14$ (red solid line), 0.1 (blue dashed line), 0.08 (cyan dash-dotted line), and 0.06 (green dotted line). Logarithmic scale for time. Straight solid line with crosses at the ends shows slope of $2/3$. $n_{1D} = 50 \mu\text{m}^{-1}$ and $T_+ = 70 \text{ nK}$ for all curves.

range of η . However, it remains unclear why this regime, which appears as asymptotic in both existing theories [20, 21], sets on after a very short time (few ms).

We now turn to the question of the decoherence time, and how it scales with the different parameters of the 1d system. In Fig. 4, we show numerically obtained values of t_0 as a function of n_{1D} . In Fig. 5, we show a plot of t_0 against the ratio n_{1D}/T_+ . We discern two different ranges of parameters. If $n_{1D}/T_+ \lesssim 1 \text{ nK}^{-1} \mu\text{m}^{-1}$, we observed a sub-exponential decay of Ψ with the value of α from the interval between 0.66 and 0.69 . The corresponding decay time is fitted by the formula

$$t_0 \approx 6.4 \frac{\hbar^3 n_{1D}^2}{m(k_B T_+)^2} = 1.6 \frac{m \lambda_T^2}{\hbar} \Big|_{T=T_+}. \quad (19)$$

Since in our calculations we took $\eta = 0.1$, and, hence, the temperature of both (+ and -) modes close to their equilibration is $T \approx 0.55 T_+$, Eq. (19) corresponds to Eq. (14) with $\kappa \approx 1.9$, which agrees by the order of magnitude with $\kappa \approx 3$ approximately evaluated in our theoretical model. Fig. 4 shows the fitting of t_0 by Eq. (19).

For $n_{1D}/T_+ \gtrsim 1 \text{ nK}^{-1} \mu\text{m}^{-1}$, our numerical method starts to fail. We are still able to fit the contrast decay by the formula (8) with $\alpha \geq 0.7$, but the corresponding values of t_0 do not obey Eq. (19) anymore, and we have instead $t_0 \approx (m/\hbar) \lambda_T^{1.67} b^{0.33}$, where the length b depends on the grid size, thus indicating a numerical artefact. A possible explanation of such a behavior is that for small temperatures and high densities the interwell coherence persists for a long time, and the numerical error in simulations accumulates faster than the actual “physical” dephasing occurs, thus yielding the dephasing time dependence on the grid size. This explanation, yet not fully corroborated, is at least in accordance with the ac-

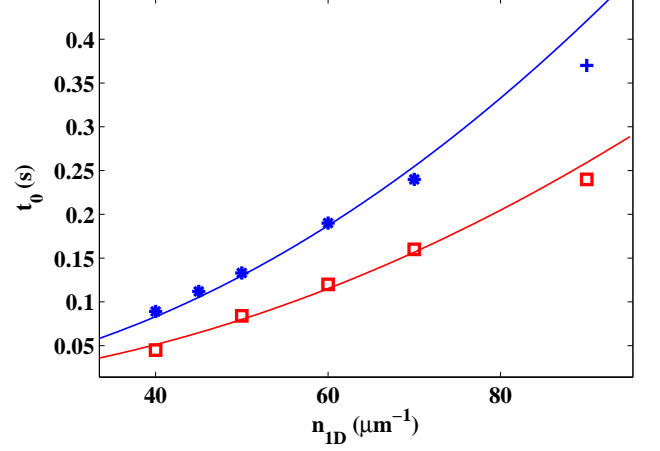


FIG. 4: (Color online). Dephasing time t_0 as a function of mean density n_{1D} for different values of temperature T_+ . Symbols: simulation results, thin line: Eq. (19). $T_+ = 70 \text{ nK}$ (blue asterisks and cross), and 90 nK (red squares).

celerated ($\alpha > 0.7$) decay of simulated coherence in the problematic parameter range. The blue cross in Fig. 4 corresponds to a parameter set from this regime.

In the case where $k_B T_+ > \mu$, t_0 starts to deviate from Eq. (19). The reason is that the theory resulting in Eq. (14) or (19) is based on the assumption that only the phononic part of the Bogoliubov spectra is occupied. This case corresponds to the first two leftmost values of Fig. 5.

In the range of applicability of Eq. (19), we checked the independence of our result on the interaction strength, see Fig. 6 for a plot of Ψ for different values of radial trapping. The only differences visible in this comparison result from statistical fluctuations. This independence of the time evolution of the coherence factor on the interaction strength confirms the validity of the theoretical model proposed in Ref. [21].

C. Correlation function

Additionally, we investigated correlation properties of the interwell coherence, which are an important tool of understanding the quasicondensate properties [14, 31, 32]. Knowing the interwell coherence autocorrelation function one can, under Gaussian fluctuation assumption, numerically construct distribution of the coherence factor (and the associated phase of the integrated interference pattern) for any sampling length. In contrast to these previous works, we deal now with non-stationary correlation properties. We express the autocorrelation function of the interwell coherence via a new function $\Phi(z - z', t)$ as

$$\langle \hat{\psi}_1^\dagger(z) \hat{\psi}_2(z) \hat{\psi}_2^\dagger(z') \hat{\psi}_1(z') \rangle \equiv n_{1D}^2 \exp(-\Phi), \quad (20)$$

Φ being determined mainly by phase fluctuations (density fluctuations are suppressed by inter-atomic repulsion

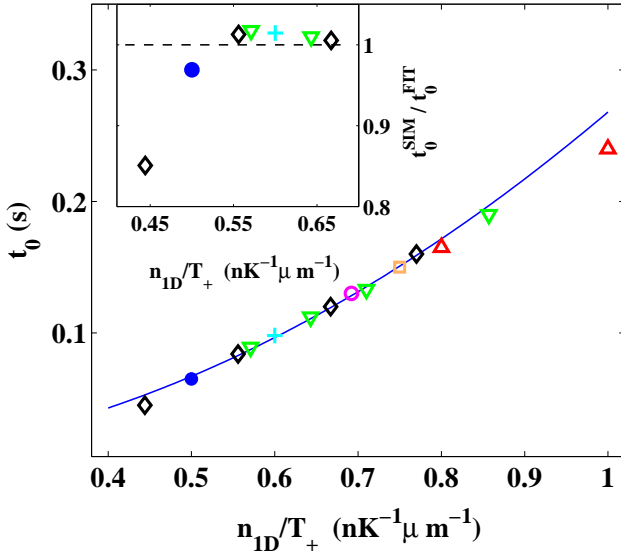


FIG. 5: (Color online). Dephasing time t_0 as a function of the ratio n_{1D}/T_+ . Solid blue line: Equation (19). Symbols: simulation results, up triangles: $T_+ = 50$ nK, square: $T_+ = 60$ nK, open circle: $T_+ = 65$ nK, down triangles: $T_+ = 70$ nK, cross: $T_+ = 75$ nK, filled circle: $T_+ = 80$ nK, diamonds: $T_+ = 90$ nK. Inset: the ratio of numerically obtained values of t_0 to the values of t_0 given by the fitting Eq. (19). The deviation of this ratio by 15% from unity (horizontal dashed line) for the leftmost point is due to temperature high enough to significantly populate particle-like states and thus violate the assumption of the phononic dispersion law underlying Eq. (19). The next point shows the same tendency, but to less extent.

in the phononic regime). Analogously to Eq. (7), we may write

$$\Phi = -\frac{1}{2} \langle [\varphi_1(z, t) - \varphi_2(z, t) - \varphi_1(z', t) + \varphi_2(z', t)]^2 \rangle. \quad (21)$$

We calculate the right-hand-side of Eq. (21) by generalizing the formula obtained by Whitlock and Bouchoule [31], where we set the interwell tunnel coupling to zero and assume that, in the transient regime, mean population of each antisymmetric mode is given by its own temperature $T_k(t)$, which depends on the mode momentum $\hbar k$ and evolves in time approximately as [21]

$$T_k(t) = \frac{T_- - T_+}{2} \exp(-\Gamma_k t) + \frac{T_- + T_+}{2} \quad (22)$$

[cf. Eq. (13), where $\eta = \frac{T_-}{T_+} \ll 1$ is neglected]. Thus we write

$$\Phi = \frac{2}{\pi} \int_0^\infty dk \frac{m k_B T_k(t)}{\hbar^2 n_{1D}} (1 - \cos k|z - z'|). \quad (23)$$

We expand $\cos k|z - z'|$ in series in powers of its argument, perform integration over k for each term expressing the integrals via the gamma-function $\Gamma(s) = \int_0^\infty dx e^{-x} x^{s-1}$

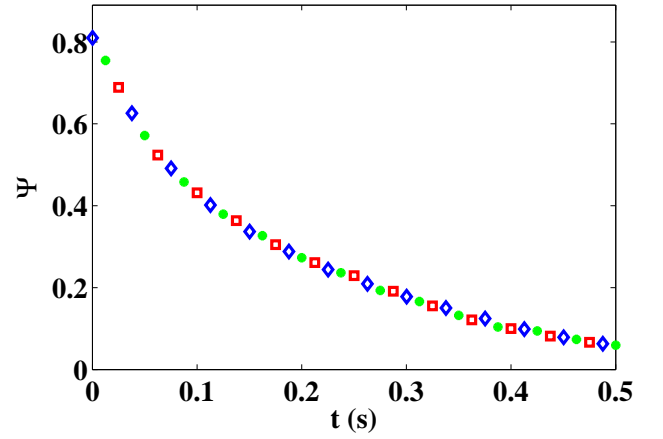


FIG. 6: (Color online). $\Psi(t)$ for several values of radial trapping frequency ω_r , $n_{1D} = 50 \mu\text{m}^{-1}$ and $T_+ = 70$ nK. $\omega_r = 2\pi \times 3$ kHz (blue diamonds), $2\pi \times 6$ kHz (green asterisks), and $2\pi \times 9$ kHz (red squares).

and re-assemble the obtained terms into hypergeometric series

$${}_nF_m(b_1, \dots, b_n; c_1, \dots, c_m; x) = 1 + \frac{b_1 b_2 \dots b_n}{c_1 c_2 \dots c_m} \frac{x}{1!} + \frac{b_1(b_1+1)b_2(b_2+1) \dots b_n(b_n+1)}{c_1(c_1+1)c_2(c_2+1) \dots c_m(c_m+1)} \frac{x^2}{2!} + \dots$$

Finally, we arrive at the following expression:

$$\Phi = \frac{2|z - z'|}{\lambda_T} \left[1 - \frac{4(1-\eta)}{3\pi(1+\eta)} \Xi(|z - z'|/a) \right], \quad (24)$$

where λ_T is to be evaluated at the equilibrated temperature $T \equiv T_\infty = (T_+ + T_-)/2$. The new auxiliary function Ξ depends on $\tilde{z} = |z - z'|/a$ only, where

$$a = \left(\frac{k_B T_\infty \zeta^2 t^2}{m n_{1D}} \right)^{1/3}. \quad (25)$$

Ξ can be expressed via hypergeometric series as follows:

$$\begin{aligned} \Xi(\tilde{z}) = & \frac{1}{\tilde{z}} \left\{ \frac{\Gamma(\frac{2}{3})\tilde{z}^2}{2} {}_3F_4 \left(\frac{1}{6}, \frac{5}{12}, \frac{11}{12}; \frac{1}{2}, \frac{5}{6}, \frac{7}{6}, \frac{4}{3}; -\frac{4}{729}\tilde{z}^6 \right) - \right. \\ & \frac{\tilde{z}^4}{24} {}_4F_5 \left(\frac{1}{2}, \frac{3}{4}, 1, \frac{5}{4}; \frac{5}{6}, \frac{7}{6}, \frac{4}{3}, \frac{3}{2}, \frac{5}{3}; -\frac{4}{729}\tilde{z}^6 \right) + \\ & \left. \Gamma\left(-\frac{2}{3}\right) \times \right. \\ & \left. \left[1 - {}_3F_4 \left(-\frac{1}{6}, \frac{1}{12}, \frac{7}{12}; \frac{1}{6}, \frac{1}{2}, \frac{2}{3}, \frac{5}{6}; -\frac{4}{729}\tilde{z}^6 \right) \right] \right\}. \end{aligned} \quad (26)$$

Φ changes significantly on a time scale t_0 . At $t = 0$ we have $\Phi = [4\eta/(1+\eta)]\lambda_T^{-1}|z - z'| \ll |z - z'|/\lambda_T$. In the opposite limit $t \gg t_0$ we have $a \rightarrow \infty$, $\tilde{z} \rightarrow 0$ for any finite coordinate difference, $\Xi \rightarrow 0$, and therefore $\Phi = 2|z - z'|/\lambda_T$.

An important advantage of the autocorrelation function (20) is its independence of the global phase diffusion

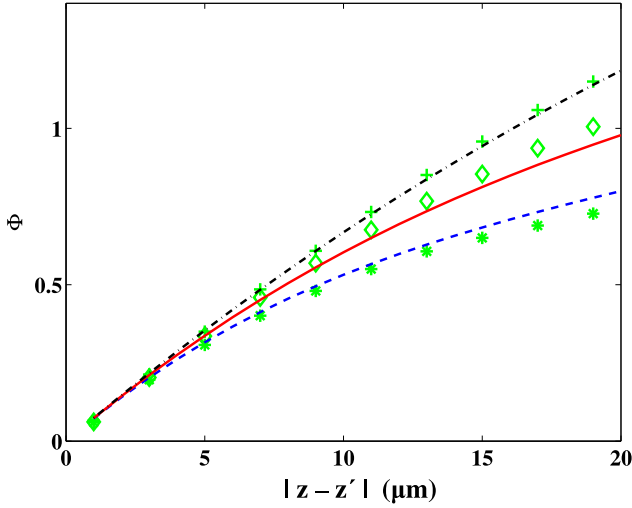


FIG. 7: (Color online). Function Φ (dimensionless) that defines the autocorrelation function of the interwell coherence Eq. (20) vs. the co-ordinate difference. Special symbols: numerical simulation results. Lines: fitting with $\varsigma = 1.0$. The quasicondensate parameters are $n_{1D} = 40 \mu\text{m}^{-1}$, $T_+ = 30 \text{ nK}$. The time elapsed after the end of coherent splitting process is $t = 0.1 \text{ s}$ (asterisks, dashed line), 0.2 s (diamonds, solid line), and 0.5 s (crosses, dot-dashed line).

[19, 29, 30]. Therefore the theoretical predictions for the autocorrelation function (20) admit direct comparison to experiment, unlike the contrast Ψ , which needs a correction to the phase diffusion. If the latter effect can not be neglected, the direct comparison of experiment to theory in terms of the contrast Ψ is hindered, because unambiguous reconstruction of the global phase shift from the measurements *in each experimental run* is practically very difficult.

In Fig. 7 we display the simulated values of Φ and their fitting by Eqs. (24 – 26) at various times t . The only fitting parameter is ς whose value is found to be $\varsigma \approx 1.0$, which is in a fair agreement with the value $\varsigma \approx 0.74$ that corresponds to the numerical prefactor in Eq. (19) and is not too far from the estimated value $\varsigma = 0.446$.

D. Comparison to experiment

In the experiment [22] the temperature T_{in} *before* splitting was known, and the temperature T_f after splitting and equilibration between the $+$ and $-$ modes was estimated using the theory of Ref. [20]. Now we repeat the same procedure using our Eq. (19). Recalling that $\eta \ll 1$, we estimate $T_f \approx 0.5 T_+$, where T_+ is obtained from Eq. (19) where t_0 is given by the experiment for certain T_{in} and n_{1D} and present the results in Fig. 8. Surprisingly, the values of T_f estimated from two models [20] and [21] are quite close to each other and are similar to T_{in} . The radial frequency range employed in [22] (from $2\pi \times 3.3 \text{ kHz}$ to $2\pi \times 4 \text{ kHz}$) is too narrow to allow

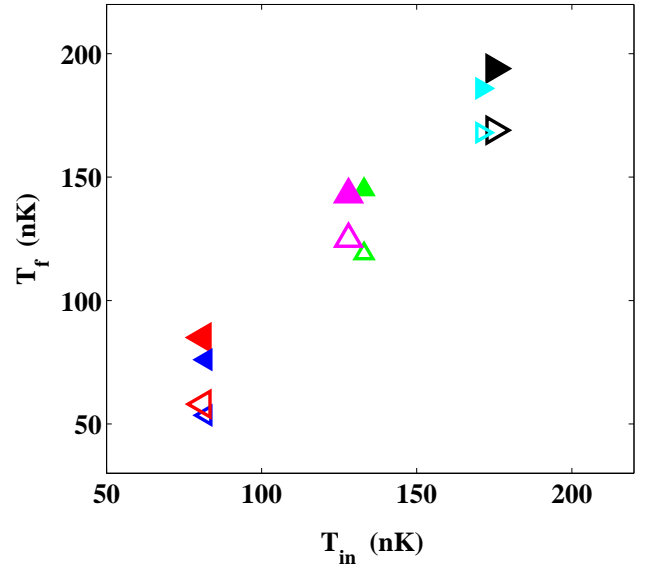


FIG. 8: (Color online). Final temperature after equilibrating in experiment extrapolated by Eq. (19) (open triangles) and by theory of Ref. [20] (filled triangles). At radial frequency $2\pi \times 3.3 \text{ kHz}$ (smaller symbols): background density $n_{1D} = 20$ (left triangles), 34 (up triangles), and $52 \mu\text{m}^{-1}$ (right triangles). At radial frequency $2\pi \times 4.0 \text{ kHz}$ (larger symbols): background density $n_{1D} = 22$ (left triangles), 37 (up triangles), and $51 \mu\text{m}^{-1}$ (right triangles).

unambiguous determination of the dependence of t_0 on ω_r .

Relation between T_+ and T_{in} under adiabatic splitting conditions

Obtaining the relation between T_+ and T_{in} is a subtle matter, not covered by the existing theories. Here we propose a way to estimate the ratio T_+/T_{in} from simple considerations. The adiabaticity of the splitting process means that the entropy (but not the energy) is conserved. In other words, populations of the momentum states should not change in the course of splitting. Just after the splitting most of the noise occurs in the symmetric mode. However, the speed of sound in the $+$ mode changes, as we show below.

Indeed, the speed of sound c is to be calculated from the formula

$$mc^2 = \frac{4\pi\hbar^2 a_s}{m} \int dx \int dy |\Psi_{\perp}(x, y)|^4 n_{\text{tot}}, \quad (27)$$

where $\Psi_{\perp}(x, y)$ is the wave function (normalized to 1) of the ground state of transverse trapping Hamiltonian. To lowest order, we neglect the influence of the atomic interactions on the transverse profile of the quasicondensate [10], in agreement with our assumption of a truly 1D regime. Eq. (27) applies for both single- and double-

well potential shape, $n_{\text{tot}} = 2n_{1\text{D}}$ being the *total* linear density of atoms in the system.

The fundamental frequency of the transverse trapping potential is ω_r before splitting. Therefore initially

$$\Psi_{\perp}^{\text{in}}(x, y) = (\sqrt{\pi}l_r)^{-1} \exp[-(x^2 + y^2)/(2l_r^2)]. \quad (28)$$

The splitting is designed so that in the end the fundamental frequency of the radial oscillations in each of the two waveguides is again ω_r . Therefore,

$$\Psi_{\perp}^{\text{as}}(x, y) \approx [\Psi_{\perp}^{\text{in}}(x - w, y) + \Psi_{\perp}^{\text{in}}(x + w, y)]/\sqrt{2} \quad (29)$$

is to be substituted into Eq. (27) to determine the speed of sound after splitting. The separation $2w$ between the two waveguides is so large that the overlap between the wave functions localized near $x = \pm w$, $y = 0$ is negligible, as it must be in the zero-tunneling case. From Eqs. (27 – 29) one can easily see that the speed of sound drops after splitting by $\sqrt{2}$.

As we discussed before, adiabatic splitting conserves the mode populations. If the temperature is comparable to the chemical potential, phonon-like modes (with the energy linearly proportional to the speed of sound) dominate. For each momentum $\hbar k$ the ratio $\hbar c|k|/T$ should be the same before and after the splitting (we denote the respective values of the speed of sound by c_{in} and c_{as}). Therefore, we expect

$$\frac{T_+}{T_{\text{in}}} = \frac{c_{\text{as}}}{c_{\text{in}}} = \frac{1}{\sqrt{2}}. \quad (30)$$

However, T_+ can be affected by non-adiabatic effects, which are far beyond our 1D approach, such as heating via creation of vortices in the course of splitting and their subsequent decay [33] or heating by technical noise.

Therefore it is extremely difficult to reliably predict *a priori* the ratio T_+/T_{in} and, moreover, $T_{\text{f}}/T_{\text{in}}$.

V. CONCLUSION

To conclude, we simulated numerically the evolution of two coherently-split quasicondensates in a broad range of experimentally feasible densities, temperatures, and effective 1D coupling strengths (radial trapping frequencies). We reproduced the subexponential decay Eq. (8) of the interwell coherence with α very close to observed [22] and theoretically predicted [20, 21] value $2/3$. Our characteristic dephasing time t_0 varies quadratically with the ratio of the linear density to the temperature (as long as $k_{\text{B}}T$ is smaller than the chemical potential and thus only the phonon part of the elementary excitation spectrum is thermally excited) and does not depend on the 1D coupling strength. The latter fact has its static counterpart – the independence of thermal phase-coherence length λ_T of a quasicondensate on the speed of sound c [13], see Eq. (5). In other words, the typical dephasing time scales as $t_0 \sim m\lambda_T^2/\hbar$, in accordance with our model [21]. This conclusion is corroborated by analysis of autocorrelation of the interwell coherence during the dephasing process. Although comparison to the experiment [22] does not show the clear preference of one of the two theories [20, 21] over another, our numerical simulations in a broad range of parameters unambiguously support our theory [21].

This work was supported by the the FWF (projects Z118-N16, P22590-N16, and SFB “VICOM”), by the WWTF (projects MA-45 and MA-07), and by the EC (STREP MIDAS).

-
- [1] W. H. Zurek and J. P. Paz, *Nuovo Cimento B* **110**, 611 (1995); M. Arndt and A. Zeilinger, *Physikalische Blätter* **56** (No. 3), 69 (2000).
 - [2] W. H. Zurek, *Rev. Mod. Phys.* **75**, 715 (2003).
 - [3] T. Pellizzari, S. A. Gardiner, J. I. Cirac, and P. Zoller, *Phys. Rev. Lett.* **75**, 3788 (1995); D. A. Lidar, I. L. Chuang, and K. B. Whaley, *Phys. Rev. Lett.* **81**, 2594 (1998); D. P. DiVincenzo, in: *Scalable Quantum Computers: Paving the Way to Realization* (eds. S. L. Braunstein, H.-K. Lo and P. Kok), Wiley-VCH Verlag, Weinheim (2005).
 - [4] R. Folman, P. Krüger, J. Schmiedmayer, J. Denschlag, and C. Henkel, *Adv. At. Mol. Opt. Phys.* **48**, 263 (2002); J. Fortágh and C. Zimmermann, *Rev. Mod. Phys.* **79**, 235 (2007); A. H. van Amerongen, *Ann. de Physique* **33**, 1 (2008).
 - [5] T. Kinoshita, T. Wenger, and D. S. Weiss, *Nature* **440**, 900 (2006).
 - [6] E. H. Lieb and W. Liniger, *Phys. Rev.* **130**, 1605 (1963); E. H. Lieb, *Phys. Rev.* **130**, 1616 (1963).
 - [7] M. Olshanii, *Phys. Rev. Lett.* **81**, 938 (1998).
 - [8] I. E. Mazets, T. Schumm, and J. Schmiedmayer, *Phys. Rev. Lett.* **100**, 210403 (2008); I. E. Mazets and J. Schmiedmayer, *New J. Phys.* **12**, 055023 (2010).
 - [9] A. Muryshev, G. V. Shlyapnikov, W. Ertmer, K. Sengstock, and M. Lewenstein, *Phys. Rev. Lett.* **89**, 110401 (2002).
 - [10] L. Salasnich, A. Parola, and L. Reatto, *Phys. Rev. A* **65**, 043614 (2002).
 - [11] I. Bouchoule, K. V. Kheruntsyan, and G. V. Shlyapnikov, *Phys. Rev. A* **75**, 031606(R) (2007).
 - [12] F. D. M. Haldane, *Phys. Rev. Lett.* **47**, 1840 (1981).
 - [13] V. N. Popov, *Functional Integrals and Collective Excitations*, Cambridge Univ. Press, Cambridge (1987); C. Mora and Y. Castin, *Phys. Rev. A* **67**, 053615 (2003).
 - [14] H.-P. Stimming, N. J. Mauser, J. Schmiedmayer, and I. E. Mazets, *Phys. Rev. Lett.* **105**, 015301 (2010).
 - [15] D. S. Petrov, G. V. Shlyapnikov, and J. T. M. Walraven, *Phys. Rev. Lett.* **87**, 050404 (2001).
 - [16] A. Imambekov, I. E. Mazets, D. S. Petrov, V. Gritsev, S. Manz, S. Hofferberth, T. Schumm, E. Demler, and J. Schmiedmayer, *Phys. Rev. A* **80**, 033604 (2009).

- [17] S. Dettmer *et al.*, Phys. Rev. Lett. **87**, 160406 (2001); D. Hellweg *et al.*, Appl. Phys. B **73**, 781 (2001); H. Kreutzmann *et al.*, Appl. Phys. B **76**, 165 (2003).
- [18] S. Manz *et al.*, Phys. Rev. A **81**, 031610 (2010).
- [19] M. Lewenstein and L. You, Phys. Rev. Lett. **77**, 3489 (1996).
- [20] A. A. Burkov, M. D. Lukin, and E. Demler, Phys. Rev. Lett. **98**, 200404 (2007).
- [21] I. E. Mazets and J. Schmiedmayer, Eur. Phys. J. B **68**, 335 (2009).
- [22] S. Hofferberth, I. Lesanovsky, B. Fischer, T. Schumm, and J. Schmiedmayer, Nature **449**, 324 (2007).
- [23] W. Bao, N.J. Mauser, and H.P. Stimming, Comm. Math. Sci. **1**, 809 (2003).
- [24] A. Polkovnikov and V. Gritsev, Nature Phys. **4**, 477 (2008).
- [25] A. Sinatra, C. Lobo, and Y. Castin, J. Phys. B **35**, 3599 (2002).
- [26] R. Bistritzer and E. Altman, Proc. Nat. Ac. Sci. USA **104**, 9955 (2007).
- [27] B. A. Wichmann and I. D. Hill, Appl. Statist. **31**, 188 (1982).
- [28] T. Kitagawa, S. Pielawa, A. Imambekov, J. Schmiedmayer, V. Gritsev and E. Demler, Phys. Rev. Lett. **104**, 255302 (2010).
- [29] J. Javanainen and M. Wilkens, Phys. Rev. Lett. **78**, 4675 (1997).
- [30] A. J. Leggett and F. Sols, Phys. Rev. Lett. **81**, 1344 (1998).
- [31] N. K. Whitlock and I. Bouchoule, Phys. Rev. A **68**, 053609 (2003).
- [32] S. Hofferberth, I. Lesanovsky, T. Schumm, A. Imambekov, V. Gritsev, E. Demler, and J. Schmiedmayer, Nature Phys. **4**, 489 (2008).
- [33] C. De Grandi, R. A. Barankov, and A. Polkovnikov, Phys. Rev. Lett. **101**, 230402 (2008); R. G. Scott, D. A. W. Hutchinson, T. E. Judd, and T. M. Fromhold, Phys. Rev. A **79**, 063624 (2009); R.G. Scott and D.A.W. Hutchinson, arXiv:0908.2930.